

Selective and Stable Non-Noble-Metal Intermetallic Compound Catalyst for the Direct Dehydrogenation of Propane to Propylene

Yang He,[‡] Yuanjun Song,[‡] David A. Cullen,[¶] and Siris Laursen^{*,‡}

[‡]Department of Chemical and Biomolecular Engineering, University of Tennessee, Knoxville, Tennessee 37996, United States [¶]Materials Science and Technology Division and Center for Nanophase Materials Sciences, Oak Ridge National Laboratory, Oak Ridge, Tennessee 37831, United States

Supporting Information

A non-noble intermetallic compound catalyst consisting of Ni₃Ga nanoparticles supported on Al₂O₃ that exhibits high selectivity (\sim 94%), comparable activity (TOF = $4.7 \times 10^{-2} \text{ s}^{-1}$), good stability (~94% to 81%) over the 82 h test), and regenerability in the direct dehydrogenation of propane to propylene at 600 °C has been developed. Through synthesis techniques that stabilize the Ni₃Ga phase, the surface composition of the catalytic nanoparticles could be tuned by Ni and Ga loading such that improved selectivity toward propylene may be achieved. Comparisons with well-defined silicasupported Ni₃Ga and NiGa catalysts and Ni₃Ga/Al₂O₃ with a range of Ni:Ga loading suggested that a specific surface composition range was most promising for propylene production. The presence of Ni at the active particle surface was also found to be critical to drive dehydrogenation and enhance conversion, whereas the presence of Ga was necessary to attenuate the reactivity of the surface to improve selectivity and catalyst stability.

Production and functionalization of unsaturated hydro-carbons (olefins and aromatics) are foundational to the chemical industry. The reactivity of unsaturated hydrocarbons makes them highly valuable yet also difficult to produce efficiently. 1-6 Catalysts for olefins/aromatics production often suffer from low selectivity due to improperly tuned surface chemistry toward reactant and product, which leads to unselective consumption of products. ^{2,4-11} Many are also still composed of expensive noble metals. ^{1,2,12-14} In an effort to improve these processes, new and inexpensive catalysts that exhibit appreciably tunable surface chemistry and low reactivity toward olefins/aromatics are needed. Changes in chemical feedstocks recently have further underscored these needs. 2,3,5,15 Herein, we focus on the discovery and development of a non-noble-metal Ni+Ga-based intermetallic compound (IMC) catalyst for the direct dehydrogenation of propane to propylene.

Catalytic materials that have achieved some degree of success in direct propane dehydrogenation for propylene production are composed of platinum IMCs and metal oxides. Pt-based IMCs, such as Pt+Sn, Pt+Ga, Pt+In, etc., exhibit activity and selectivity, but are still comprised of expensive metals, suffer from sintering, and require Cl₂ regenerative treatments. 2,3,16-18 Several non-noble-metal oxides, such as

CrO_x, VO_x, MoO_x, GaO_x, etc., also exhibit activity and selectivity in alkane dehydrogenation reactions, yet suffer from the loss of oxygen under reaction conditions, rapid deactivation, and require frequent regeneration treatments.^{2,19–25}

Herein, we present the discovery of a stable and selective propane dehydrogenation catalyst consisting of aluminasupported (70% delta, 30% gamma phase) phase-pure Ni₃Ga IMC nanoparticles with Ga-rich surfaces (actual loading Ni:Ga 1:1, particle size average of 11.2 nm). Through new synthesis techniques, the most stable IMC phase of Ni₃Ga could be kinetically promoted and trapped despite off-stoichiometric actual Ni:Ga loading. This tunability enabled the production of the high-performance main catalyst. However, due to the use of alumina as an oxide support, some Ga was trapped on the oxide surface and left unincorporated into the IMC nanoparticles, leading to a less well-defined core-shell-like IMC nanoparticle composition. This complexity limited the determination of the IMC surface composition through highsensitivity, low energy ion scattering spectroscopy (HS-LEIS), yet was avoided when a silica support was employed. Comparison of the main catalyst to well-defined, phase-pure, bulk-like-terminated silica-supported catalysts of Ni₃Ga/SiO₂ and NiGa/SiO2, and Ni3Ga/Al2O3 catalysts with a range of actual Ni:Ga loadings, helped to suggest the active and selective composition of the main catalyst.

Many complexities were presented in developing the synthesis procedures for the supported IMC catalysts, too many to outline fully in a Communication. However, a brief overview of the understanding is presented to aid in reproducing our results. Ni and Ga as nitrate salts were loaded on alumina using a hydroxide method and on silica by incipient wetness. In the hydroxide method, Ni and Ga nitrate were transformed to their hydroxides in H₂O using dilute NaOH. The pre-catalysts were then subjected to a reductive treatment to form the IMC particles. Annealing under Ar at 700 °C for 12 h was applied to select catalysts to grow IMC particle size and manipulate IMC surface composition. The bulk crystal phase of the Ni+Ga IMC particles was found to be sensitive to the reactivity of the oxide surface and the concentration of H₂ and temperature employed during reduction. These effects were traced back to the diffusion

Received: May 14, 2018 Published: October 16, 2018



Journal of the American Chemical Society

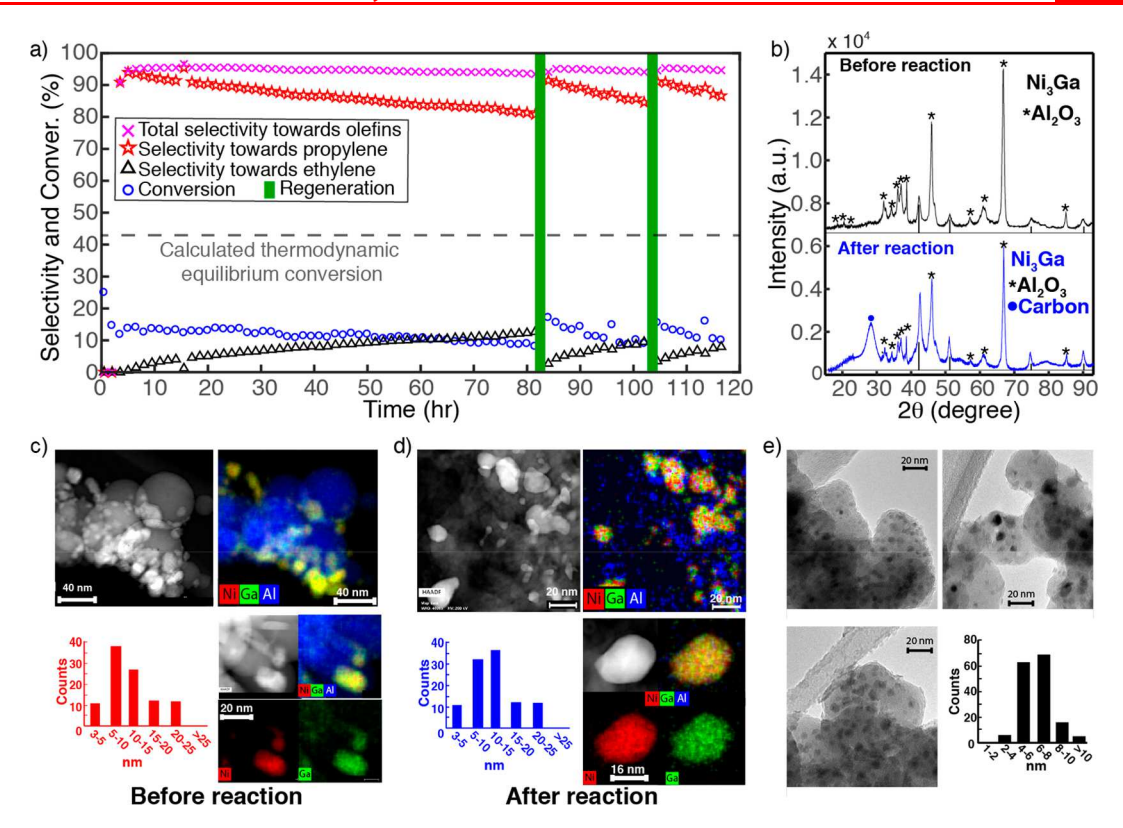


Figure 1. (a) Catalytic activity, 82 h stability, and regenerability of $(1:1 \text{ Ni:Ga})@\text{Ni}_3\text{Ga}/\text{Al}_2\text{O}_3$. (b) HR-pXRD of $(1:1 \text{ Ni:Ga})@\text{Ni}_3\text{Ga}/\text{Al}_2\text{O}_3$ before and after reaction (c,d) HAADF and EDX per-particle elemental mapping over $(1:1 \text{ Ni:Ga})@\text{Ni}_3\text{Ga}/\text{Al}_2\text{O}_3$ before and after reaction. (e) BF-TEM of annealed Ni₃Ga/SiO₂.

and availability of Ga during IMC particle formation and the kinetic preference for Ni₃Ga formation.

When an alumina support was utilized, lower concentrations of $\rm H_2$ and lower temperatures led to the preferential formation of the $\rm Ni_3Ga$ phase, yet also resulted in some amount of Ga remaining on the oxide surface, unincorporated in the IMC particles due to the reactivity of alumina (Figures 1b and S1). Employing silica, a less reactive support, allowed for nearly all Ga loaded to be incorporated into the IMC particles. This phenomenon enabled the production of catalysts that consisted of either $\rm Ni_3Ga$ particles with tunable surface composition over alumina (2% $\rm H_2$ for 1 h at 500 °C) or bulk-like terminated $\rm Ni_3Ga$ or $\rm NiGa$ particles over either support (100% $\rm H_2$ at 700 °C for 2 h for alumina and 10% $\rm H_2$ at 700 °C for 2 h for silica, see Figures 2 and S2–S4).

Annealing treatments under Ar at 700 °C for 12 h were used to grow IMC particle size and found not to affect the bulk phase of the IMCs (Figure S6). For the silica-supported catalysts, this treatment also aided in driving the surface composition to be bulk-like (Figure 2b). The effect of annealing on the surface composition of the alumina-supported catalysts could not be determined because of the effect of unincorporated Ga. For the alumina-supported catalysts that exhibited bulk crystal phases that differed from actual Ni and Ga loading, the naming convention of (actual loading element ratio)@particle-bulk-phase/oxide-support is utilized, e.g., (1:1 Ni:Ga)@Ni₃Ga/Al₂O₃. This naming convention does not imply an exact IMC surface composition. ICP-OES measurements confirmed that actual loadings were within a few percent of target loadings (Table S1). Ni+Ga IMC crystal phase was found to be particle-size-independent. Co-feed of H2 was not employed in any of our tests. We note that the offstoichiometric composition at the surface of the aluminasupported particles was un-detectable via XRD.

The main catalyst of the study, (1:1 Ni:Ga)@Ni₃Ga/Al₂O₃, exhibited high steady-state selectivity towards propylene production (~94%) using only Ar-diluted propane. Stability was appreciable, with only moderate deactivation in long-term performance tests at 600 °C (~94% to 81%, Figure 1a). Conversion remained moderately stable as well (~13% to 9%) over the 82 h test. Ethylene, another valuable olefin, was the only other major product. Selectivity towards total olefin production was nearly constant at ~94%. Methane and ethane were minor products (Figures S7 and S8). Regeneration was possible through in situ O2 and H2 treatment. Comparison with published catalytic performance of commercial catalysts, Pt-Sn (Oleflex, 80-91% selectivity at 25-40% conversion under 1.2-2 bar) and CrO_x (CATOFIN, 80-90% selectivity at 48-65% conversion under 0.3-1.0 bar), as well as with in-houseproduced Pt-Sn and CrO_r catalysts (Figures S9 and S10), indicated that (1:1 Ni:Ga)@Ni₃Ga/Al₂O₃ exhibited comparable or higher selectivity and stability.^{26–30}

Turnover frequency (TOF) rates for the catalysts were determined using chemisorption of $\rm H_2$ or CO to determine reaction site concentration for overall rate normalization (see Figure S11 for isothermal plots). The TOF rate of 4.7 \times 10^{-2} s $^{-1}$ for propylene production over (1:1 Ni:Ga)@Ni_3Ga/Al_2O_3 was comparable to or greater than the TOF rates for the inhouse-synthesized catalysts of Pt+Sn (4.5 \times 10^{-2} s $^{-1}$) or CrO $_x$ (1.3 \times 10^{-3} s $^{-1}$) and within an order of magnitude of published results for Pt+Sn and CrO $_x$ (Table S2). $^{24,31-34}$ TOF values of industrial catalysts could not be found in the literature or patents.

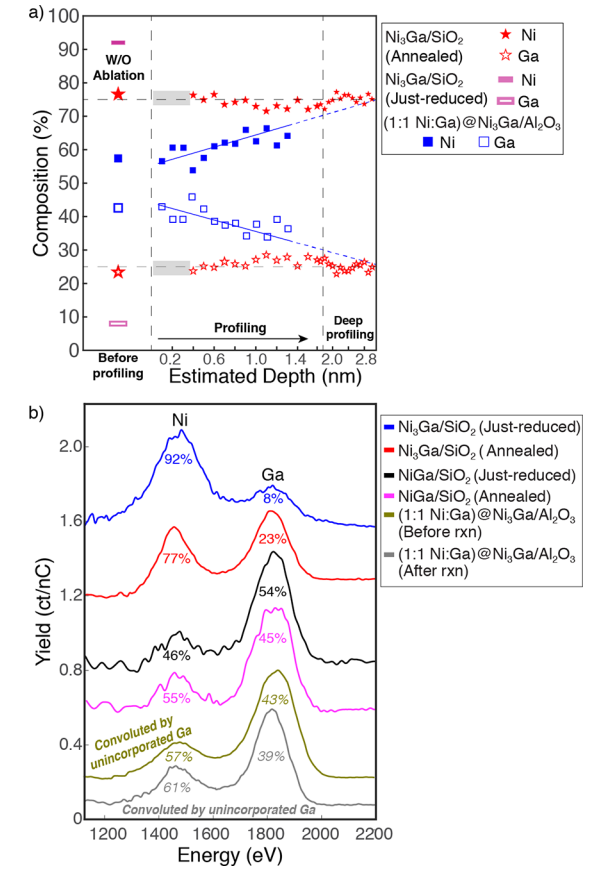


Figure 2. (a) HS-LEIS depth-profiling of annealed Ni₃Ga/SiO₂ (red) and as-prepared (1:1 Ni:Ga)@Ni₃Ga/Al₂O₃ (blue); gray boxes mark where signal-to-noise ratio affected the HS-LEIS data. (b) HS-LEIS of just-reduced Ni₃Ga/SiO₂ (blue), annealed Ni₃Ga (red), just-reduced NiGa (black), annealed NiGa (magenta), and (1:1 Ni:Ga)@Ni3Ga/ Al₂O₃ before (olive) and after reaction (gray).

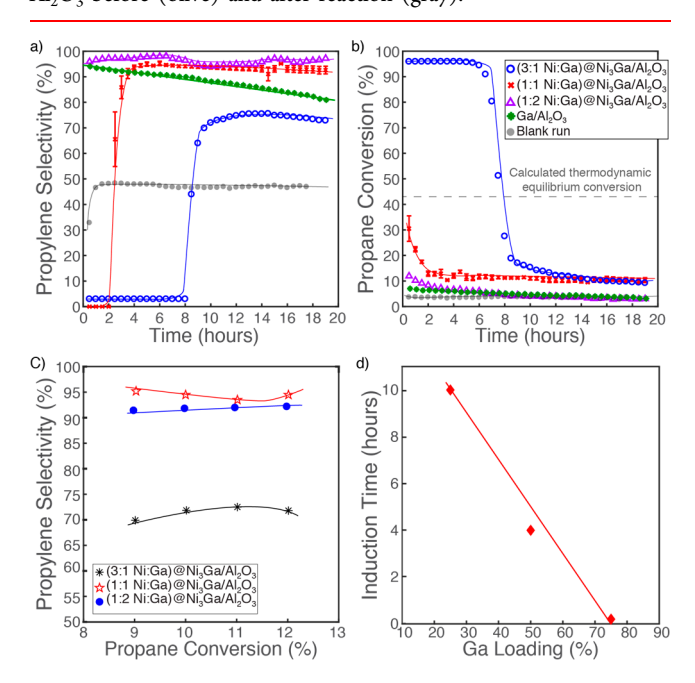


Figure 3. Catalytic performance of propane dehydrogenation over Ni₃Ga/Al₂O₃ with different Ni:Ga actual loadings.

Post-reaction catalyst characterization indicated the IMC nanoparticles were surprisingly stable. XRD showed phasepure Ni₃Ga persisted with no new phases present. TEM indicated little change in particle size or morphology (average 11.2 nm to average of 12.5 nm). Coke formation as carbon nanotubes was found to be selectively present about the main catalyst and associated with smaller IMC particles (Figure \$12). Expulsion of Ga and the formation of Ni carbide in less stable small particles may be responsible for the coke formation, but this was not directly investigated.

Efforts to capture the surface composition of the main catalyst using HS-LEIS such that it may be correlated with catalytic performance failed due to the presence of unincorporated Ga on the oxide surface. Therefore, connections between IMC surface composition and catalytic performance were instead derived through comparison with well-defined phase-pure silica-supported catalysts where the IMC surface composition could be measured reliably. The suite of silica-supported catalysts consisted of phase-pure Ni₃Ga and NiGa in just-reduced and annealed states. EDS analysis of these samples showed that the majority of Ga was incorporated into the IMC particles. Depth profiling of the annealed Ni₃Ga/SiO₂ sample was used to calibrate the HS-LEIS data. The measured surface concentrations of Ni and average particle sizes of the well-defined catalysts were 92% and 4.3 nm, 77% and 6.8 nm, 46% and 3.6 nm, and 55% (particle size not determined) for just-reduced Ni₃Ga, annealed Ni₃Ga, just-reduced NiGa, and annealed NiGa, respectively, with the balance of the composition being Ga (Figure 2b). HS-LEIS depth profiling data for the main catalyst is presented for completeness, which showed an approach to the bulk Ni₃Ga composition, but profiling was stopped before this value was reached.

Activity tests for just-reduced Ni₃Ga/SiO₂ catalyst yielded no presentable data, as deactivation and significant coke production occurred within the first hour. This indicated that the Ni-rich surface or smaller average particle size of this catalyst was responsible for driving unselective reactions. The annealed Ni₃Ga/SiO₂, where the surface composition was bulk-like (77% Ni and 23% Ga), showed measurable activity over 3.5 h but exhibited mostly unselective activity and rapid deactivation (Figure S15a). The annealed NiGa/SiO₂ displayed selectivity (82%) and stability similar to those of the main catalyst yet exhibited lower conversion (Figure S16). These results demonstrated that a systematic increase in propylene selectivity was directly connected to elevated concentrations of Ga at the Ni+Ga IMC surface. An alumina-supported NiGa catalyst with phase-pure NiGa particles and Ni:Ga loading of 1:1 was also prepared and tested. This catalyst is expected to be Ga-lean at the NiGa particle surface. Its performance showed selectivity comparable $(\sim 90+\%)$ to that of the main catalyst, but it deactivated more rapidly (Figure S16). Comparison of the catalytic performance between SiO₂-supported Ni+Ga IMCs and (1:1 Ni:Ga)@ Ni₃Ga/Al₂O₃ suggested that a surface composition between 3:1 and 1:1 Ni:Ga was potentially responsible for favorable performance of the main catalyst. An IMC particle size effect is also likely present, yet was not studied directly.

Because the Ni₃Ga phase could be preferentially stabilized despite off-stoichiometric actual loadings of Ni and Ga, a suite of catalysts that consisted of Ni:Ga of 3:1, 1:1 (the base case), and 1:2 actual loadings were prepared and tested. Because some Ga is lost on the oxide surface, the IMC particles are expected to be lean in Ga in comparison to actual Ga loading. A systematic reduction in the induction time was observed as Ga loading increased, suggesting that over-reactive surface sites were being modified or blocked by Ga. At a Ni:Ga ratio of 2:1, conversion was reduced. Similar trends have been observed for noble-metal IMC catalysts^{35,36} and in well-defined surface science studies of olefin adsorption.^{37–39} Systematic improvement of selectivity and reduction in conversion suggest that some concentration of Ni must be present at the IMC surface to drive the reaction, yet too much Ni leads to surface chemistry that drives unselective propane conversion. Catalyst loading in the reactor was then modified to investigate conversion vs selectivity effects. As selectivity was not a strong function of conversion, the performance of the catalysts could not be ascribed simply to lower conversion (Figure 3c).

Non-noble-metal IMC catalysts present a relatively new compositional space that exhibits unique surface and catalytic chemistry which is promising for olefin production. Through the current understanding of their synthesis as supported nanoparticles, well-defined and tunable bulk and surface compositions could be achieved and their catalytic activity tuned. Results suggest that a surface composition between 3:1 Ni:Ga and 1:1 Ni:Ga is responsible for the high performance of the (1:1 Ni:Ga)@/Ni₃Ga/Al₂O₃ catalyst. Further investigations are needed to fully understand the nature of the IMC surface reaction sites, yet the attenuation of surface reactivity that leads to elevated selectivity toward propylene production was nonetheless achieved.

ASSOCIATED CONTENT

S Supporting Information

The Supporting Information is available free of charge on the ACS Publications website at DOI: 10.1021/jacs.8b05060.

Experimental details, including synthesis, reactor test, TEM, EDS, HS-LEIS, pXRD and HR-pXRD, ICP-OES, and chemisorption (PDF)

AUTHOR INFORMATION

Corresponding Author

*slaursen@utk.edu

ORCID ®

Siris Laursen: 0000-0002-5769-7393

Notes

The authors declare no competing financial interest.

ACKNOWLEDGMENTS

This research was supported by the National Science Foundation (NSF) CAREER award (Grant CBET-1752063) and the ACS PRF award (PRF# 57589-ND5). TEM, EDX, and regular XRD analysis were conducted at the Center for Nanophase Materials Sciences (CNMS project number CNMS2017-151 and CNMS2017-156) at Oak Ridge National Lab (ORNL), which is a US Department of Energy Office of Science User Facility. This work utilized the Advanced Photon Source for HR-XRD analysis at Argonne National Laboratory supported by the U.S. Department of Energy, Office of Science, Office of Basic Energy Sciences, under Contract No. DE-AC02-06CH11357. This work used the Extreme Science and Engineering Discovery Environment (XSEDE), which was supported by the National Science Foundation grant number ACI-1053575. The authors also

acknowledge the kind help of Henry Luftman at Lehigh University for assistance in LEIS.

REFERENCES

- (1) Han, Z.; Li, S.; Jiang, F.; Wang, T.; Ma, X.; Gong, J. Nanoscale 2014, 6, 10000.
- (2) Sattler, J. J. H. B.; Ruiz-Martinez, J.; Santillan-Jimenez, E.; Weckhuysen, B. M. Chem. Rev. 2014, 114, 10613–10653.
- (3) Sattler, J. J. H. B.; Gonzalez-Jimenez, I. D.; Luo, L.; Stears, B. A.; Malek, A.; Barton, D. G.; Kilos, B. A.; Kaminsky, M. P.; Verhoeven, T. W. G. M.; Koers, E. J.; Baldus, M.; Weckhuysen, B. M. *Angew. Chem., Int. Ed.* **2014**, 53, 9251–9256.
- (4) Vajda, S.; Pellin, M. J.; Greeley, J. P.; Marshall, C. L.; Curtiss, L. A.; Ballentine, G. A.; Elam, J. W.; Catillon-Mucherie, S.; Redfern, P. C.; Mehmood, F.; Zapol, P. *Nat. Mater.* **2009**, *8*, 213–216.
- (5) McFarland, E. Science 2012, 338, 340-342.
- (6) Wang, H.; Cong, Y.; Yang, W. Chem. Commun. 2002, 14, 1468-1469
- (7) Chen, M.; Xu, J.; Cao, Y.; He, H. Y.; Fan, K. N.; Zhuang, J. H. J. Catal. 2010, 272, 101–108.
- (8) He, Y.; Laursen, S. ACS Catal. 2017, 7, 3169-3180.
- (9) Kundakovic, L.; Flytzani-Stephanopoulos, M. J. Catal. 1998, 179, 203–221.
- (10) He, Y.; Laursen, S. Catal. Sci. Technol. 2018, 8, 5302-5314.
- (11) Xiong, K.; Lee, W. S.; Bhan, A.; Chen, J. G. ChemSusChem 2014, 7, 2146–2149.
- (12) Pham, H. N.; Sattler, J. J. H. B.; Weckhuysen, B. M.; Datye, A. K. ACS Catal. 2016, 6, 2257–2264.
- (13) Iglesias-Juez, A.; Beale, A. M.; Maaijen, K.; Weng, T. C.; Glatzel, P.; Weckhuysen, B. M. J. Catal. 2010, 276, 268–279.
- (14) Galvita, V.; Siddiqi, G.; Sun, P.; Bell, A. T. *J. Catal.* **2010**, *271*, 209–219.
- (15) Conti, J. J.; Holtberg, P. D.; Beamon, J. A.; Napolitano, S. A.; Schaal, M.; Turnure, J. T. Annual Energy Outlook 2013, DOE/EIA-0383(2013); U.S. Energy Information Administration, April 2013; https://www.eia.gov/outlooks/aeo/pdf/0383(2013).pdf (accessed October 9, 2018).
- (16) Ballarini, A. D.; Zgolicz, P.; Vilella, I. M.; de Miguel, S. R.; Castro, A. A.; Scelza, O. A. *Appl. Catal.*, A **2010**, 381, 83–91.
- (17) Lee, M.; Nagaraja, B.; Lee, K.; Jung, K. Catal. Today 2014, 232, 53–62.
- (18) Xia, K.; Lang, W.; Li, P.; Yan, X.; Guo, Y. RSC Adv. 2015, 5, 64689-64695.
- (19) Airaksinen, S. M. K.; Harlin, M. E.; Krause, A. O. I. *Ind. Eng. Chem. Res.* **2002**, *41*, 5619–5626.
- (20) Chen, M.; Xu, J.; Su, F.; Liu, Y.; Cao, Y.; He, H.; Fan, K. J. Catal. 2008, 256, 293–300.
- (21) Lopez Cordero, R.; Gil Llambias, F.; Lopez Agudo, A. Appl. Catal. 1991, 74, 125–136.
- (22) Hakuli, A.; Harlin, M.; Backman, L.; Krause, A. J. Catal. 1999, 184, 349-356.
- (23) Harlin, M.; Backman, L.; Krause, A.; Jylhä, O. *J. Catal.* **1999**, 183, 300–313.
- (24) Puurunen, R. J. Catal. 2002, 210, 418-430.
- (25) Takahara, I.; Saito, M.; Inaba, M.; Murata, K. Catal. Lett. 2004, 96, 29–32.
- (26) Nawaz, Z. Rev. Chem. Eng. 2015, 31, 413-436.
- (27) CATOFIN Dehydrogenation, 03M082014H_v2; McDermott International, Inc., April 2018; https://www.cbi.com/getattachment/9c663848-b4ae-4c51-b51a-49db1154c47f/CATOFIN-Dehydrogenation.aspx (accessed October 9, 2018).
- (28) Maddah, H. Am. Sci. Res. J. Eng. Technol. Sci. 2018, 45, 49-63.
- (29) Zhao, P.; Guan, Y.; Wang, Y.; Guo, X.; Zhang, J.; Du, Z.; Zhang, S.; Xie, Q.; Wu, S. IOP Conf. Ser.: Mater. Sci. Eng. 2017, 167, 012053.
- (30) Petroleum. UOP Oleflex Process for Light Olefin Production, https://pet-oil.blogspot.com/2012/10/uop-oleflex-process-for-light-olefin.html (accessed October 9, 2018).

- (31) Duan, Y.; Zhou, Y.; Zhang, Y.; Sheng, X.; Xue, M. Catal. Lett. **2011**, 141, 120–127.
- (32) Bariås, O. A.; Holmen, A.; Blekkan, E. A. J. Catal. 1996, 158, 1–12.
- (33) Salmones, J.; Wang, J. A.; Galicia, J. A.; Aguilar-Rios, G. J. Mol. Catal. A: Chem. **2002**, 184, 203–213.
- (34) Sattler, J. J. H. B.; González-Jiménez, I. D.; Mens, A. M.; Arias, M.; Visser, T.; Weckhuysen, B. M. Chem. Commun. 2013, 49, 1518.
- (35) Wang, G.; Zhang, H.; Wang, H.; Zhu, Q.; Li, C.; Shan, H. J. Catal. 2016, 344, 606-608.
- (36) Zhang, Y.; Zhou, Y.; Qiu, A.; Wang, Y.; Xu, Y.; Wu, P. Catal. Commun. 2006, 7, 860–866.
- (37) Zhao, H.; Koel, B. E. Surf. Sci. 2004, 572, 261-268.
- (38) Xu, C.; Tsai, Y. L.; Koel, B. E. *J. Phys. Chem.* **1994**, 98, 585–
- (39) Hamm, G.; Schmidt, T.; Breitbach, J.; Franke, D.; Becker, C.; Wandelt, K. Surf. Sci. **2004**, 562, 170–182.